JOURNAL OF THERMOPHYSICS AND HEAT TRANSFER
Vol. 16, No. 1, January–March 2002

Ultrafast Laser Heating on Metal Films: Effects of Microvoids

D. Y. Tzou*
University of Missouri–Columbia, Columbia, Missouri 65211

The effect of internal voids in microfilms on the change of the surface reflectivity is analyzed. The dual-phase-lag model is employed to describe the interweaving behaviors of thermalization and relaxation during the short time transient. The normalized temperature change in the two-dimensional films containing a microvoid is obtained by an explicit algorithm of finite differencing, aiming at retrieval of the Crank–Nicholson criterion as a special case. The presence of microvoids can significantly reduce the normalized surface reflectivity change, sometimes by one order of magnitude, which has been observed experimentally.

Nomenclature

a	=	autocorrelation factor in the laser pulse, dimensionless
J	=	laser fluence, J/m^2
K	=	thermal conductivity, W/m K
L	=	thin-film thickness, m
R	=	surface reflectivity, dimensionless
S	=	energy absorption rate, W/m^3
T	=	temperature, K
t	=	physical time, s
t_p	=	laser pulse width, s
w	=	width of the square microvoid, m
x, y	=	space coordinates, m
α	=	thermal diffusivity, m^2/s
Δ	=	space or time increment
δ	=	skin depth of laser penetration, m
κ	=	wave number, dimensionless
ξ	=	amplification factor in error propagation, dimensionless
τ	=	phase lags, s

Subscripts and Superscripts

D	=	defect
i, j	=	nodal number in the $x(i)$ and $y(j)$ directions
n	=	nodal number in time sequence
q	=	heat flux
T	=	temperature gradient
0	=	initial or reference values

Introduction

FAST laser heating is central to material characterizations and laser processing of thin-film materials. Examples with demonstrated success include nondestructive evaluation of high-T_c superconducting films,[1] monitoring of grain structure and thickness of metallic films,[2] laser micromachining[3] and patterning,[4] and laser tailoring of microstructures and thin-film deposition.[5] In addition to expediting the vigorous growth of new technologies, the femtosecond lasers have also facilitated detailed studies of the fundamental phenomena in ultrafast heat transport. Validating the microscopic two-step models[6,7] and determination of dominating microstructural properties[8–10] and delay times[11–14] are direct results of increasing availability of high-power short-pulse lasers in recent years.

A submicrometer film would be more sensitive to the microstructural defects due to its comparable physical dimension (film thickness) to that of the defect. Possible forms of defects are granular dislocations, microvoids, or pin holes resulting from relative slippage during the process of film deposition. In characterizing the temperature dependence of optical properties of noble metals, in fact, the quantum-mechanical reflectivity model assuming a perfect (defect-free) film geometry[15] was found to yield a surface reflectivity change being approximately one order of magnitude larger than the experimental results.[16] Whereas all of the qualitative features were preserved well in the reflectivity model, the possible lattice defects in the gold film were believed to be a major factor resulting in such a large quantitative discrepancy, along with the uncertainties of the model parameters.

This work provides a quantitative study for the effect of the microstructural defects on the surface reflectivity of thin films in the picosecond domain of transient. To describe the interweaving behaviors of thermal relaxation and rapid thermalization during the picosecond transient, the dual-phase-lag (DPL) model that explicitly captures the thermalization time and relaxation time in the framework of thermal lagging is adopted to study the redistribution of thermal energy around a microvoid. Microstructural defects may induce anisotropic response in both thermal[17] and optical[18] applications. Although pinholes are common defects for metal films in the submicrometer range, a square hole is modeled in the two-dimensional analysis here to illustrate the general effects of the void size and location. A mixed finite difference scheme is developed for the numerical analysis, aiming at recovery of the familiar Crank–Nicholson criterion in absence of thermal lagging. The finite difference method directly computes the nodal temperatures and fluxes during the picosecond transient. Because of the blurred physical meaning of nonequilibrium temperature in the picosecond domain, however, the values of Qiu and Tien[8–10] will be normalized with respect to the maximum value that occurs in the same transient period. For metal films undergoing a temperature change less than the Debye temperature (165 K for gold, a characteristic temperature proportional to the cutoff frequency of vibratory lattices that can be assumed as a continuum), such normalized temperature change has been shown describable by the normalized reflectivity change that was measured directly by the pumping-and-probing technique at the film surfaces. To address the much lower surface reflectivity change that was observed experimentally on films with possible inclusions of defects, therefore, the normalized temperature change shall be used throughout the analysis.

Two-Dimensional Formulation

Figure 1a shows a thin film of thickness L subjected to the radiation of a short-pulse laser. The film thickness is in the submicrometer range, comparable to the grain size of metals. Granular mismatch may occur in the solidification process of the metal vapor, giving rise to microstructural defects along the grain boundaries. Because the film thickness is in the submicrometer range (assumed to be 0.1 μm later), the characteristic dimension of the microstructural defect is comparable to the film thickness, which is exemplified by

Received 28 February 2001; revision received 24 July 2001; accepted for publication 3 August 2001.

*James C. Dowell Professor, Department of Mechanical and Aerospace Engineering.

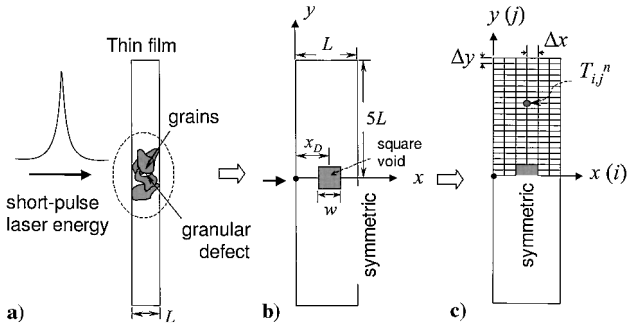

Fig. 1 Two-dimensional film subjected to the irradiation of a short-pulse laser: a) granular defect resulting from granular mismatch, b) simulation of the granular defect by a square hole in a symmetric two-dimensional film, and c) the uniform mesh used in the finite difference analysis.

a square hole of width w located at a distance x_D measured from the heated surface, as shown in Fig. 1b. The width-to-length ratio of the metal film is assumed to be 1:5, which will be sufficient to illustrate the far-field response, that is, the temperature response far away from the microvoid.

The real electron temperature is achieved after the first few hundred femtoseconds (subpicoseconds) in ultrafast laser heating.[16] The linearized DPL model is employed here to describe the combined effects of thermal relaxation and thermalization during the short-time transient,[13,19]

$$\frac{\partial^2 T}{\partial x^2}+\frac{\partial^2 T}{\partial y^2}+\tau_T\left(\frac{\partial^3 T}{\partial x^2\partial t}+\frac{\partial^3 T}{\partial y^2\partial t}\right)+\frac{1}{k}\left(S+\tau_q\frac{\partial S}{\partial t}\right)$$

$$=\frac{1}{\alpha}\frac{\partial T}{\partial t}+\frac{\tau_q}{\alpha}\frac{\partial^2 T}{\partial t^2} \tag{1}$$

where laser irradiation is described by the energy absorption rate S in the thickness x direction of the thin film,[11,13,20]

$$S(x,t)=0.94J\left(\frac{1-R}{t_p\delta}\right)\exp\left[-\left(\frac{x}{\delta}+\frac{a|t-2t_p|}{t_p}\right)\right] \tag{2}$$

which closely resembles the Gaussian distribution employed by Qiu and Tien.[8–10] The thermalization effect is absorbed in the term led by τ_T, which contains two third-order derivatives of temperature (twice in space and once in time), and the relaxation effect is absorbed in the terms led by τ_q, which involve an apparent heating term $(\partial S/\partial t)$ and a wave term $(\partial^2 T/\partial t^2)$ during the short-time transient. Because of the interweaving behaviors of thermalization (τ_T effect) and relaxation (τ_q effect), and the additional effect from the apparent heating, note that the time at which the temperature change in the film reaches a maximum will be different from the time at which the laser power reaches a maximum. Interfering by the apparent heating term due to thermal relaxation, in addition, the full width at half maximum (FWHM) along does not characterize laser heating applied to the thin film. Although Eq. (1) is introduced to describe the normalized temperature change of the electron gas in this work, it can be used equally well to describe the nonequilibrium temperature in different microsystems. When $\tau_T=\tau_q$, for example, Eq. (1) reduces to the equilibrium temperature depicted by the classical Fourier's law. When $\tau_T=0$, Eq. (1) reduces to the thermal wave equation proposed by Cattaneo[21] and Vernotte.[22,23] Other cases for different values of τ_T and τ_q in correlation to the representative models in microscale heat transfer, including the phonon scattering model, the hyperbolic two-step model, and the three-equation model, are illustrated in the works by Tzou.[13,20] Though covering several models in the same framework of thermal lagging, Eq. (1) remains to be a special form that neglects the effects of phonon waves during the ultrafast transient. This assumption is valid for ultrafast laser heating with a low intensity, which is a typical situation when used for characterizing thin metal films.[16] Under a laser fluence of 13.4 J/m^2, which will be used in the present study, the metal lattices remain almost thermally undisturbed. Along with the small change of the temperature gradient across the film, the wave effect for heat transport through phonons is indeed negligible.

Energy loss from all surfaces is negligible during the picosecond transient,[8,11,13] resulting in the following insulated conditions in accordance with the coordinate system shown in Fig. 1b:

$$\frac{\partial T}{\partial x}=0 \quad \text{at} \quad \begin{cases} x=0 \text{ (front surface) and } x=L \text{ (rear surface)} \\ x=x_D\pm\dfrac{w}{2},\ y\in\left[0,\dfrac{w}{2}\right] \text{(void surfaces)} \end{cases} \tag{3}$$

$$\frac{\partial T}{\partial y}=0 \quad \text{at} \quad y=\frac{w}{2},\ x\in\left[x_D-\frac{w}{2},x_D+\frac{w}{2}\right] \text{(void surfaces)} \tag{4}$$

Only the upper half plan ($y\geq 0$) needs to be considered due to symmetry of the problem. The symmetric conditions are imposed at $y=0$ (the x axis) and are expressed as

$$\frac{\partial T}{\partial y}=0 \quad \text{at} \quad y=0,\ x\in\left[0,x_D-\frac{w}{2}\right] \quad \text{and} \quad x\in\left[x_D+\frac{w}{2},L\right] \tag{5}$$

Employing the same condition of FWHM pulse duration, t_p, describing the temporal shape of the laser pulse, the initial time is shifted from zero to $-2t_p$ (Refs. 8–11, 13, and 20). The initial conditions at $t=-2t_p$ are, thus,

$$T=T_0, \qquad \frac{\partial T}{\partial t}=0 \tag{6}$$

where the second condition refers to a thermal disturbance from a stationary state.

Note that the symmetrical condition posed in Eq. (5), in correlation to the thin-film model containing multiple voids, is sometimes used as the periodic condition imposed on the boundaries of the unit cell enclosing a representative void.[13] The results obtained as follows, therefore, would reflect certain qualitative features in films with multiple voids in microscale. A quantitative assessment, obviously, will require implementation of such periodic conditions in all directions surrounding the representative cell (if the distribution of such microvoids is indeed uniform) or placement of individual microvoids in the computational model (for distinctive microvoids).

Finite Differencing

An explicit finite difference solution to Eqs. (1–6) will be attempted, mainly for intractable analytical solutions in the multiply connected region and because of the need for a stability and convergence criterion for the DPL equation. Although a powerful implicit scheme of finite difference already exists,[24] fulfilling this vacancy is necessary in the continuous development of the thermal lagging model.

Two-Dimensional Formulation

The stability and convergence criterion will be derived by the mixed use of central differencing, backward differencing, and forward differencing in Eq. (1), so that the resulting criterion can be explicitly reduced to the Crank–Nicholson criterion in the limiting case of Fourier diffusion. The central difference scheme, as usual, is applied to all of the second-order derivatives in space and time:

$$\left(\frac{\partial^2 T}{\partial x^2}\right)_{i,j}^n=\frac{1}{(\Delta x)^2}\left[T_{i+1,j}^n-2T_{i,j}^n+T_{i-1,j}^n\right]$$

$$\left(\frac{\partial^2 T}{\partial y^2}\right)_{i,j}^n=\frac{1}{(\Delta y)^2}\left[T_{i,j+1}^n-2T_{i,j}^n+T_{i,j-1}^n\right]$$

$$\left(\frac{\partial^2 T}{\partial t^2}\right)_{i,j}^n=\frac{1}{(\Delta t)^2}\left[T_{i,j}^{n+1}-2T_{i,j}^n+T_{i,j}^{n-1}\right] \tag{7}$$

The backward difference scheme, in time, is then applied to all of the terms containing the mixed derivatives:

$$\left(\frac{\partial^3 T}{\partial x^2 \partial t}\right)^n_{i,j} = \frac{1}{(\Delta x)^2(\Delta t)} \times \left[T^n_{i+1,j} - 2T^n_{i,j} + T^n_{i-1,j} - T^{n-1}_{i+1,j} + 2T^{n-1}_{i,j} - T^{n-1}_{i-1,j}\right]$$

$$\left(\frac{\partial^3 T}{\partial y^2 \partial t}\right)^n_{i,j} = \frac{1}{(\Delta y)^2(\Delta t)} \times \left[T^n_{i,j+1} - 2T^n_{i,j} + T^n_{i,j-1} - T^{n-1}_{i,j+1} + 2T^{n-1}_{i,j} - T^{n-1}_{i,j-1}\right] \quad (8)$$

The forward difference scheme is applied to all of the first-order derivatives in time:

$$\left(\frac{\partial T}{\partial t}\right)^n_{i,j} = \frac{1}{\Delta t}\left[T^{n+1}_{i,j} - T^n_{i,j}\right], \qquad \left(\frac{\partial S}{\partial t}\right)^n_{i,j} = \frac{1}{\Delta t}\left[S^{n+1}_{i,j} - S^n_{i,j}\right] \quad (9)$$

The stability and convergence criterion depicting the appropriate space and time increments (Δx, Δy, and Δt) is independent of the heating terms. In studying the stability and convergence criterion for Eq. (1), therefore, both the real, S, and apparent ($\partial S/\partial t$) source terms will be temporarily omitted. The error propagation of lagging temperature can be analyzed by the von Neumann eigenmode decomposition with $\iota = \sqrt{-1}$ (Ref. 25):

$$T^n_{i,j} = \xi^n \exp[\iota\kappa(i\Delta x + j\Delta y)] \quad (10)$$

When Eq. (10) is substituted into Eqs. (7–9) and the results back into Eq. (1), the amplification factor ξ can be obtained as a function of κ. The amplification factor thus obtained is a complex number. The stability condition requires that $|\xi|^2 \le 1$ for all values of κ, which can be simplified to give

$$\frac{2\alpha\Delta t(2\tau_T + \Delta t)}{(2\tau_q + \Delta t)}\left[\frac{1}{(\Delta x)^2} + \frac{1}{(\Delta y)^2}\right] \le 1 \quad (11)$$

Equation (11) must be satisfied by the grid sizes of Δx, Δy, and Δt for obtaining a convergent solution from the finite difference scheme shown in Eqs. (7–9). In the case of $\tau_T = \tau_q$, not necessarily equal to zero,[11,13] heat flux vector and temperature gradient become instantaneous and the lagging behavior diminishes. Equation (11) in this case reduces to

$$\alpha\Delta t[1/(\Delta x)^2 + 1/(\Delta y)^2] \le \tfrac{1}{2} \quad (12)$$

which is the familiar Crank–Nicholson criterion in Fourier diffusion. Note that the space grid with $\Delta x = \Delta y$ is often used in finite difference calculations. For the two-dimensional formulation, Eq. (11) in this case can be simplified as

$$\Delta x \ge \sqrt{\frac{4\alpha\Delta t(2\tau_T + \Delta t)}{2\tau_q + \Delta t}}, \qquad \Delta y = \Delta x \quad (13)$$

One-Dimensional Reduction

The stability and convergence criterion for the one-dimensional DPL equation can be derived as a special case. Denoting the one-dimensional spatial grid size by Δx and time grid size by Δt, the same procedure results in the following requirement for the one-dimensional formulation:

$$\Delta x \ge \sqrt{\frac{2\alpha\Delta t(2\tau_T + \Delta t)}{2\tau_q + \Delta t}} \quad (14)$$

The factor 4 in Eq. (13) for the two-dimensional formulation is changed to 2 in Eq. (14) for the one-dimensional formulation. Similarly, in the case of $\tau_T = \tau_q$, Eq. (14) is reduced to the one-dimensional Crank–Nicholson criterion in Fourier diffusion. Equations (11), (13), and (14) are in general forms that cover the classical thermal wave equation[21–23] with $\tau_T = 0$. For thermal waves propagating in a one-dimensional medium, the resulting criterion, $(\Delta x/\Delta t) \ge \sqrt{[2\alpha/(2\tau_q + \Delta t)]}$, which can be derived directly from Eq. (14) by setting $\tau_T = 0$, results in indistinguishable results when compared to the analytical solutions.[19,20]

Note that the DPL model [Eq. (1)] describes the microstructural effects of rapid thermalization and relaxation in terms of the resulting delayed response in time. As far as the thermalization and relaxation behaviors are concerned, no additional consideration is needed to incorporate the microstructural effects; even though the space, Δx, and time, Δt, increments in Eqs. (13) and (14) may be reduced to the orders of mean free path (time) of electrons. To describe additional effects in microscale, such as the tunneling effects of phonons or quantum effects of electrons in transporting heat, Eq. (1) needs to be modified according to the Boltzmann transport equation to accommodate such effects. An example is the T-wave model[13] that includes a jerk term (third-order derivative of temperature with respect to time) reflecting the ballistic behavior of heat transport by electrons near the Fermi surface.

Numerical Results

We first examine the one-dimensional finite difference results by comparing them to the earlier obtained analytical and experimental results. A microvoid is then introduced into the two-dimensional film to investigate the effects of void size and location on thin-film heating.

One-Dimensional Validation

A gold film of thickness 0.1 μm heated by a 96-fs (t_p) pulse laser was studied by Brorson et al.[26] and Qiu et al.[16] Figure 2 shows the normalized temperature change at the front surface ($x = 0$) of the film, which was converted from the normalized surface reflectivity measured in their experiments. The analytical result employed the Riemann-sum approximation for obtaining the lagging temperature[11–13] under the same thermal and optical properties determined for the gold film: $\alpha = 1.2 \times 10^{-4}$ m^2/s, $R = 0.93$, and $J = 13.4$ J/m^2 (Refs. 8–10). The autocorrelation factor simulating the temporal profile of the laser pulse is chosen to be $a = 1.992$, in contrast to the model parameter 2.77 assumed in the Gaussian profile that describes the normalized autocorrelation of the laser pulse in the experiment.[16] The response curve obtained at the front surface of the film accurately describes the experimental results, which

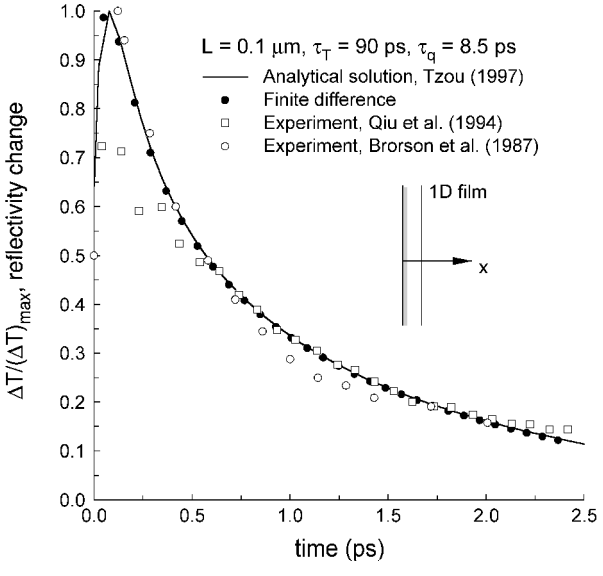

Fig. 2 Normalized temperature change at the front surface of a one-dimensional film; comparison of the finite difference solutions with the analytical and experimental results.

justifies the effective values of $\tau_T = 90$ ps and $\tau_q = 8.5$ ps for the gold film, as well as the use of the normalized temperature change in describing the normalized surface reflectivity change obtained experimentally.

The same problem is investigated by the one-dimensional finite difference algorithm developed in this work. The time increment is chosen to be $\Delta t = 8$ fs, resulting in $\Delta x \geq 4.51$ nm according to Eq. (14) for a stable and convergent solution. The finite difference results shown in Fig. 2 employ $\Delta x = 5$ nm, resulting in a transient curve that agrees well with both the analytical and experimental results.

Effects of Microvoids

For a two-dimensional film containing a square microvoid, as shown in Fig. 1c, an equal-sided ($\Delta x = \Delta y$) uniform mesh is used to discretize the physical domain. Mesh objectiveness is carefully examined by incessantly doubling the number of grid points used in the analysis, until a consistent numerical accuracy is achieved. The Cauchy norm in the successful approximation is less than 1% for all of the results presented in this work. The space and time increments are chosen to be $\Delta t = 4.5$ fs and $\Delta x = \Delta y = 5$ nm, which satisfy the criterion posed in Eq. (13).

The film thickness is assumed to be $L = 0.1\,\mu$m throughout the study. To demonstrate the pronounced effect of microvoids, we first consider a square void of 20% of the film thickness, $w/L = 0.2$ or $w = 0.02\,\mu$m, that is located at $x_D/L = 0.2$ ($x_D = 0.02\,\mu$m). Figure 3 shows the normalized temperature change obtained at different locations on the front surface ($x = 0$) of the film. In correspondence with the normalized reflectivity change measured in the experiments, the temperature change $[\Delta T(t) = T(t) - T_0]$ is normalized with respect to its maximum value, $(\Delta T)_{\max} = T_{\max} - T_0$, which occurs in the same transient period. Emphasis should be placed on the transient response after 0.5 ps, when the physical process of thermalization starts. The temperature response between 0 and 0.5 ps should be ignored because even the physical meaning of the normalized temperature change becomes blurred in this time domain. The presence of a microvoid significantly reduces the normalized temperature change at $y = 0$, which is immediately left to the microvoid. When compared to the far-field response away from the microvoid (the defect-free response), the amount of reduction may reach one order of magnitude. This confirms the suspicion raised by Qiu et al.[16] in their efforts examining the optical/thermal properties of thin metal films. While preserving the same feature in rapid thermalization, the normalized temperature change in films with a defect approaches that without (defect-free) as the distance from the microvoid increases; this is evidenced by the transient curves at $y = 0.5L$ (0.05 μm), L (0.1 μm), $2L$ (0.2 μm), and $3L$ (0.3 μm) in Fig. 3. No significant difference in the normalized temperature change can be observed for $y > 2L$, and the one-dimensional solution (defect-free, full circles shown in Fig. 2) is recovered beyond this threshold.

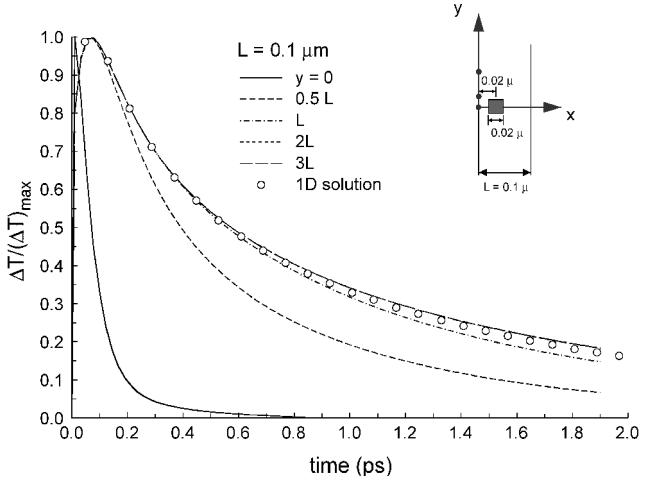

Fig. 3 Normalized temperature change at different locations on the front surface ($x = 0$) of the film containing a square microvoid: L = 0.1 μm, x_D = 0.02 μm, and w = 0.02 μm.

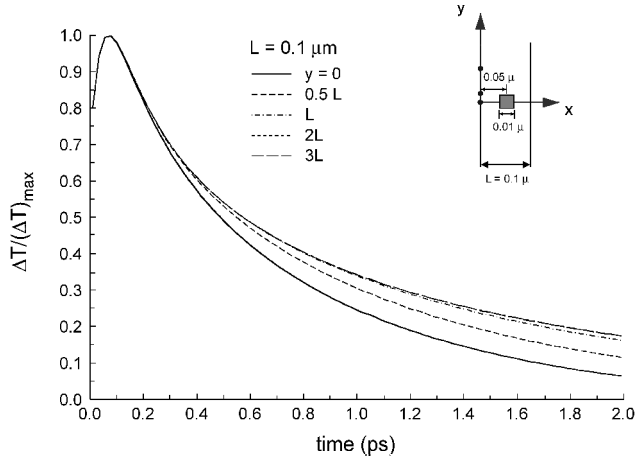

Fig. 4 Normalized temperature change at different locations on the front surface ($x = 0$) of the film containing a square microvoid: L = 0.1 μm, x_D = 0.05 μm, and w = 0.01 μm (smallest size).

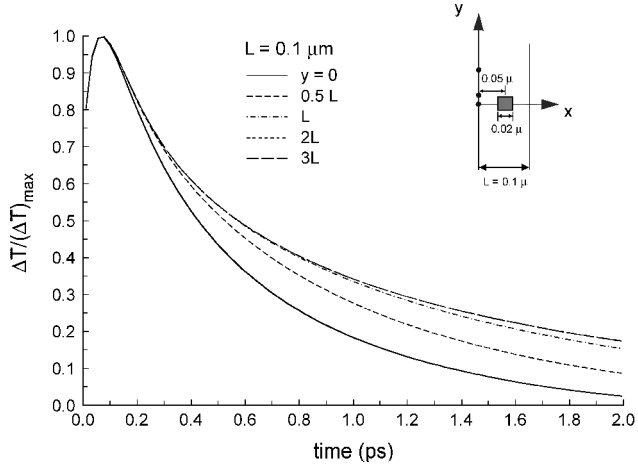

Fig. 5 Normalized temperature change at different locations on the front surface ($x = 0$) of the film containing a square microvoid: L = 0.1 μm, x_D = 0.05 μm, and w = 0.02 μm (medium size).

Reduction of the normalized temperature change depends on both size and location of the microvoid. At the same distance from the front surface, $x_D = 0.05\,\mu$m, Figs. 4–6 show the front-surface temperature for the two-dimensional film containing a microvoid of different sizes: $w = 0.01\,\mu$m (Fig. 4), 0.02 μm (Fig. 5), and 0.03 μm (Fig. 6). The effect of the microvoid diminishes, and consequently, the defect-free solutions are recovered, as $y > 2L$ (0.2 μm). Again, in all of the cases shown, the normalized temperature change can be lower than that in a defect-free film by one order of magnitude. The time at which such a significant reduction occurs, however, decreases as the microvoid size increases. For the case of $w = 0.03\,\mu$m and $y = 0$, as shown in Fig. 6, this occurs as $t \cong 1.61$ ps where the normalized surface temperature in a defective film is 0.022 in contrast to that in a perfect (defect-free) film being 0.222.

The effect of the microvoid becomes weaker as its distance from the heated surface increases, as expected. With the same size microvoid studied in Fig. 3, $w = 0.02\,\mu$m, the distance of the microvoid is increased from $x_D = 0.03\,\mu$m (Fig. 7) to 0.08 μm (Fig. 8) to illustrate such a distance effect. When compared to Fig. 3 ($x_D = 0.02\,\mu$m), the normalized temperature changes shown in Fig. 7 are higher at all of the corresponding values of y because the microvoid is farther away from the heated front surface ($x_D = 0.03\,\mu$m). This becomes even more obvious in Fig. 8, where the microvoid is moved close to the rear surface, $x_D = 0.08\,\mu$m. The

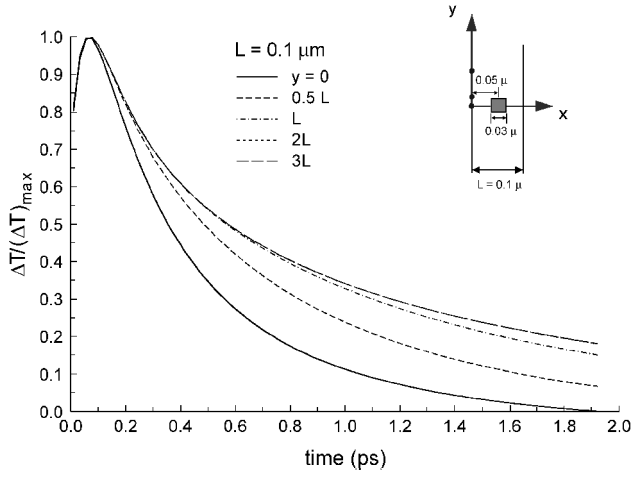

Fig. 6 Normalized temperature change at different locations on the front surface ($x = 0$) of the film containing a square microvoid: $L = 0.1$ μm, $x_D = 0.05$ μm, and $w = 0.03$ μm (largest size).

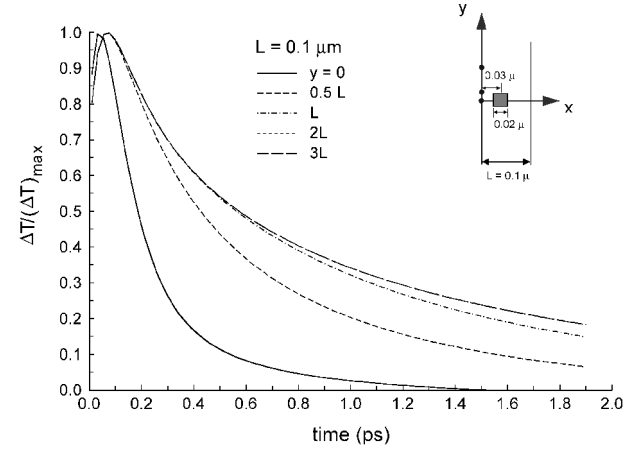

Fig. 7 Normalized temperature change at different locations on the front surface ($x = 0$) of the film containing a square microvoid: $L = 0.1$ μm, $w = 0.02$ μm, and $x_D = 0.03$ μm (medium position).

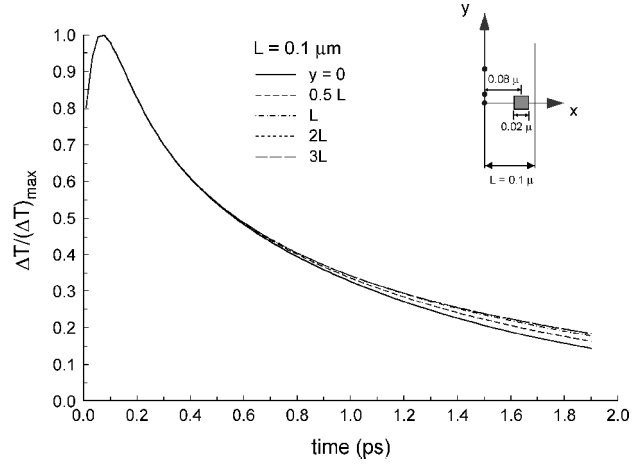

Fig. 8 Normalized temperature change at different locations on the front surface ($x = 0$) of the film containing a square microvoid: $L = 0.1$ μm, $w = 0.02$ μm, and $x_D = 0.08$ μm (farthest position).

normalized temperature changes at different locations on the front surface (different values of y) are not only higher, but also closer to each other in comparison with those in Figs. 3 and 7 due to the weaker effect of the microvoids.

The presence of a microvoid with insulated surfaces, regardless of its shape, results in higher values of both $T(t)$ (the transient temperature at the front surface) and $T_{\max}$ [the maximum value of $T(t)$ in the same transient period] due to the reduced areas in transporting heat through the film. When compared to the case of a perfect film without any defects, a smaller value of the normalized temperature change, that is, $\Delta T/(\Delta T)_{\max} = [T(t) - T_0]/[T_{\max} - T_0]$ shown in Figs. 3–8, implies a larger increase of $T_{\max}$ than $T(t)$ from T_0. The resulting temperature response of $T_{\max}$, in other words, is more exaggerated than $T(t)$ in the presence of a microvoid. Along with the local intensification of thermal energy around a microvoid,[13] the significant reduction of the normalized temperature change (and, hence, the normalized reflectivity change) is a noteworthy effect of microvoids.

The finite difference scheme developed in this work has been extended to incorporate the effect of temperature-dependent thermal properties in Ref. 27.

Conclusions

The effect of microvoids during the short-time transient in ultrafast laser heating has been quantified in this work. The emphasis has been placed on the microstructural effects on the normalized temperature change, which is a quantity directly correlated to the normalized surface reflectivity change measured from the pumping-and-probing technique. Microvoids have been confirmed as an internal structure to reduce the normalized temperature change on the film surface. The actual reduction depends on both the size and the location of the microvoid in the thin film. A larger microvoid (size effect) or a microvoid closer to the heated surface (location effect) would result in a normalized temperature change that is lower than that in a perfect (defect-free) film by one order of magnitude. This is consistent with the earlier observations.

A mixed, explicit finite difference scheme has been developed to solve the linearized DPL equation that describes the interwoven behaviors of thermal relaxation and thermalization at short times. The stability and convergence criterion is derived by the von Neumann eigenmode analysis, which dictates the appropriate space and time increments for a reliable numerical solution. In absence of thermal lagging, such a criterion reduces to the classical Crank–Nicholson criterion in Fourier diffusion. This criterion should be applicable to a number of other microscopic models, including the phonon scattering model and the three-equation model in microscale heat transfer inasmuch as the field equations in these models have the same form as the DPL equation. The use of the mixed formation in terms of both heat flux and temperature, due to the temperature-dependent thermal diffusivity, effective heat capacity, and thermalization and relaxation times, necessitates constant updates of thermal properties in the heating history that add significant complexities in the numerical procedure. Following the same stability and convergence criterion derived in this work, however, the surface reflectivity agrees very well with the experimental results for thin films of various thickness.

References

[1] Mandelis, A., and Peralta, S. B., "Thermal-Wave Based Materials Characterization and Nondestructive Evaluation of High-Temperature Superconductors: A Critical Review," *Physics and Materials Science of High Temperature Superconductors II*, edited by R. Kossowsky, B. Raveau, D. Wohlleben, and S. Patapis, Kluwer Academic, Boston, 1992, pp. 413–440.

[2] Opsal, J., "The Application of Thermal Wave Technology to Thickness and Grain Size Monitoring of Aluminum Films," *Metallization: Performance and Reliability Issues for VLSI and ULSI*, Vol. 1596, Society of Photo-Optical Instrumentation Engineers, Bellingham, WA, 1991, pp. 120–131.

[3] Knapp, J. A., Børgesen, P., and Zuhr, R. A. (eds.), "Beam–Solid Interactions: Physical Phenomena," *Materials Research Society Symposium and Proceedings*, Vol. 157, Materials Research Society, Pittsburgh, PA, 1990.

[4] Elliott, D. J., and Piwczyk, B. P., "Single and Multiple Pulse Ablation of Polymeric and High Density Materials with Excimer Laser Radiation at 193 nm and 248 nm," *Materials Research Society Symposium and Proceedings*, Vol. 129, 1989, pp. 627–636.

[5] Grigoropoulos, C. P., "Heat Transfer in Laser Processing of Thin Films," *Annual Review of Heat Transfer*, edited by C. L. Tien, Vol. 5, Hemisphere, New York, 1994, pp. 77–130.

[6] Kaganov, M. I., Lifshitz, I. M., and Tanatarov, M. V., "Relaxation Between Electrons and Crystalline Lattices," *Soviet Physics—JETP*, Vol. 4, No. 4, 1957, pp. 173–198.

[7] Anisimov, S. I., Kapeliovich, B. L., and Perel′man, T. L., "Electron

Emission from Metal Surfaces Exposed to Ultra-Short Laser Pulses," *Soviet Physics—JETP*, Vol. 39, No. 2, 1974, pp. 375–377.

[8]Qiu, T. Q., and Tien, C. L., "Short-Pulse Laser Heating on Metals," *International Journal of Heat and Mass Transfer*, Vol. 35, No. 3, 1992, pp. 719–726.

[9]Qiu, T. Q., and Tien, C. L., "Heat Transfer Mechanisms During Short-Pulse Laser Heating of Metals," *Journal of Heat Transfer*, Vol. 115, Nov. 1993, pp. 835–841.

[10]Qiu, T. Q., and Tien, C. L., "Femtosecond Laser Heating of Multi-Layered Metals—I. Analysis," *International Journal of Heat and Mass Transfer*, Vol. 37, No. 17, 1994, pp. 2789–2797.

[11]Tzou, D. Y., "A Unified Field Approach for Heat Conduction from Micro- to Macro-Scales," *Journal of Heat Transfer*, Vol. 117, No. 1, 1995, pp. 8–16.

[12]Tzou, D. Y., "Experimental Support for the Lagging Response in Heat Propagation," *Journal of Thermophysics and Heat Transfer*, Vol. 9, No. 4, 1995, pp. 686–693.

[13]Tzou, D. Y., *Macro- to Microscale Heat Transfer: The Lagging Behavior*, Taylor and Francis, Washington, DC, 1997.

[14]Tzou, D. Y., and Chen, J. K., "Thermal Lagging in Random Media," *Journal of Thermophysics and Heat Transfer*, Vol. 12, No. 4, 1998, pp. 567–574.

[15]Rosei, R., "Temperature Modulation of the Optical Transmissions Involving the Fermi Surface in Ag: Theory," *Physical Review B: Solid State*, Vol. 10, 1974, pp. 474–483.

[16]Qiu, T. Q., Juhasz, T., Suarez, C., Bron, W. E., and Tien, C. L., "Femtosecond Laser Heating of Multi-Layered Metals—II. Experiments," *International Journal of Heat and Mass Transfer*, Vol. 37, No. 17, 1994, pp. 2799–2808.

[17]Flik, M. I., and Tien, C. L., "Size Effect on the Thermal Conductivity of High-T_C Thin-Film Superconductors," *Journal of Heat Transfer*, Vol. 112, 1990, pp. 872–881.

[18]Hodgkinson, I. J., and Wilson, P. W., "Microstructural-Induced Anisotropy in Thin Films for Optical Applications," *CRC Critical Reviews in Solid State and Materials Sciences*, Vol. 15, No. 1, 1988, pp. 26–28.

[19]Chiu, K. S., "Temperature Dependent Properties and Microvoids in Thermal Lagging," Ph.D. Dissertation, Univ. of Missouri, Columbia, MO, 1999.

[20]Tzou, D. Y., "Ultrafast Heat Transport: The Lagging Behavior," Society of Photo-Optical Instrumentation Engineers 44th Annual Meeting and Exhibition, Invited Paper, July 1999.

[21]Cattaneo, C., "A Form of Heat Conduction Equation Which Eliminates the Paradox of Instantaneous Propagation," *Compte Rendus*, Vol. 247, 1958, pp. 431–433.

[22]Vernotte, P., "Les Paradoxes de la Théorie Continue de l′équation De La Chaleur," *Compte Rendus*, Vol. 246, 1958, pp. 3154, 3155.

[23]Vernotte, P., "Some Possible Complications in the Phenomena of Thermal Conduction," *Compte Rendus*, Vol. 252, 1961, pp. 2190, 2191.

[24]Joshi, A. A., and Majumdar, A., "Transient Ballistic and Diffusive Phonon Heat Transport in Thin Films," *Journal of Applied Physics*, Vol. 74, 1993, pp. 31–39.

[25]Press, W. H., Teukolsky, S. A., Vetterling, W. T., and Flannery, B. P., *Numerical Recipes*, 2nd ed., Cambridge Univ. Press, New York, 1992, pp. 827–830.

[26]Brorson, S. D., Fujimoto, J. G., and Ippen, E. P., "Femtosecond Electron Heat-Transport Dynamics in Thin Gold Film," *Physical Review Letters*, Vol. 59, 1987, pp. 1962–1965.

[27]Tzou, D. Y., and Chiu, K. S., "Temperature-Dependent Thermal Lagging in Ultrafast Laser Heating," *International Journal of Heat and Mass Transfer*, Vol. 44, No. 9, 2001, pp. 1725–1734.